ACS Catalysis

Research Article

pubs.acs.org/acscatalysis

Effect of Pre-Reduction on the Properties and the Catalytic Activity of Pd/Carbon Catalysts: A Comparison with Pd/Al_2O_3

Giovanni Agostini,[*,†,‡] Carlo Lamberti,[†,¶] Riccardo Pellegrini,[§] Giuseppe Leofanti,[∥] Francesco Giannici,[⊥] Alessandro Longo,[⊗,▽] and Elena Groppo[†]

[†]Department of Chemistry, INSTM Reference Center and NIS Centre of Excellence, Università di Torino, Via P. Giuria 7, I-10125 Torino, Italy

[‡]European Synchrotron Radiation Facility, 6 Rue Jules Horowitz, F-38600 Grenoble, France

[¶]CrisDI Interdepartmental Center for Crystallography, University of Turin, Italy

[§]Chimet SpA-Catalyst Division, Via di Pescaiola 74, I-52041 Viciomaggio, Arezzo, Italy

[∥]Consultant, Via Firenze 43, 20010 Canegrate, Milano, Italy

[⊥]Dipartimento di Fisica e Chimica, Università di Palermo, viale delle Scienze, I-90128 Palermo, Italy

[⊗]Netherlands Organization for Scientific Research at ESRF, BP 220, F-38043 Grenoble Cedex 9, France

[▽]Istituto per lo Studio dei Materiali Nanostrutturati del CNR, Via Ugo La Malfa 153, I-90146 Palermo, Italy

ABSTRACT: The effect of pre-reduction in solution with chemical reagents on the catalytic performance and catalyst properties of Pd/carbon catalysts was systematically investigated with a multitechnique approach. The results are critically discussed in comparison to those recently obtained on analogous Pd/alumina catalysts. It was proved that the Pd phase on the carbon surface is characterized by a high mobility, opposite to what occurs on alumina. As a result, the Pd particles on carbon aggregate together during pre-reduction, with a consequent decrease in available metal surface. Pd particles remain aggregated also in reaction conditions; the decreased Pd dispersion negatively affects the catalyst activity in the debenzylation of 4-benzyloxyphenol.

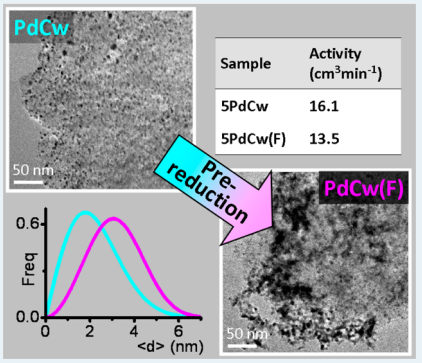

KEYWORDS: *Pd-based catalysts, heterogeneous catalysis, characterization techniques, temperature-programmed reduction, CO chemisorption, TEM, X-ray Absorption Spectroscopy, Small Angle X-ray Spectroscopy*

1. INTRODUCTION

Pre-reduction in solution with chemical reagents is a common step in the preparation of Pd-based heterogeneous catalysts,[1,2] although its role is far from being understood. In the attempt to correlate catalyst properties and catalytic performance, we recently investigated the effects of pre-reduction in solution by chemical reagents on a Pd/Al_2O_3 catalyst.[3] We demonstrated that pre-reduction has two major effects. First, the supported Pd phase, although still partially oxidized, is more easily reducible than in the corresponding unreduced catalyst; thus, the induction period during the debenzylation of 4-benzyloxyphenol is negligible. Second, the Pd nanoparticles obtained in reducing conditions are different from those formed on the unreduced catalyst: slightly bigger and more regular (both in the bulk and on the surface), and more embedded into the Al_2O_3 support, as a consequence of a partial mobility of the Al_2O_3 support in the reducing environment. As a consequence, a structure-sensitive reaction such as the debenzylation of 4-benzyloxyphenol is favored (i.e., the activity increases).[3]

We successively continued our investigation by performing a similar study on Pd-based carbon-supported catalysts. The chemical-physical properties of activated carbons, which are by far the most used supports for Pd-based catalysts, are completely different from those of metal-oxide supports, such as Al_2O_3.[4−10] As a result, the supported Pd phase is likely to be different in the two cases, although the preparation method is the same. A pre-reduced Pd/C catalyst does not show the same catalytic performance as the corresponding unreduced catalyst,[2,9−14] suggesting that pre-reduction affects the catalyst state. As a matter of fact, in some cases it is more convenient to use an unreduced catalyst,[11,12,15] whereas in other cases a pre-reduced catalysts shows better performance.[1,2] In general, pre-reduction increases the stability of Pd/C catalysts toward leaching.[1,2] It is thus interesting to investigate the effects of pre-reduction on the properties of the Pd/C catalysts in terms of oxidation state of the supported Pd phase and its reducibility, and of the properties of the final Pd nanoparticles. A clear correlation among these factors (oxidation state and reducibility

Received: July 4, 2013
Revised: September 11, 2013
Published: October 29, 2013

   dx.doi.org/10.1021/cs400507m | *ACS Catal.* 2014, 4, 187−194

of PdO_x supported phase, properties of Pd nanoparticles, and catalytic performance) is not present in literature. Herein, we apply the same set of experimental tools successfully employed in the characterization of Pd/Al_2O_3 catalysts (i.e., TPR, XAS, TEM, and SAXS),[4,16−19] and we correlate the above-mentioned properties with the catalytic performance in the same debenzylation reaction already tested on Pd/Al_2O_3.[3]

2. EXPERIMENTAL SECTION

2.1. Catalyst Preparation and Nomenclature. Supported Pd samples were prepared in the Chimet Laboratories on a wood-based activated carbon (surface area = 980 $m^2\ g^{-1}$; pore volume = 0.62 $cm^3\ g^{-1}$), following the deposition-precipitation method, with Na_2PdCl_4 as palladium precursor and Na_2CO_3 as basic agent,[4] Pd loadings in the 0.5−5.0 wt % range were used. All catalysts were carefully washed until complete Cl^- removal was achieved and then they were kept in their wet state (ca. 50% of water) until measurement. No Pd was found in the solution after filtration (as determined by ICP). For the 5.0 wt % catalyst, after the deposition of palladium as hydroxide and before Cl^- removal, pre-reduction was carried out by means of three different reducing agents, that is, HCOONa, $NaBH_4$, or hydrogen. In all cases, pre-reduction was performed at 338 K for 1 h; with hydrogen, the treatment was performed inside a stainless steel autoclave, under 10 bar of pressure. As for unreduced catalysts, the reduced ones were successively water-washed until residual Cl^- were completely removed and then stored in their wet state; also in this case the washing solution did not contain any Pd. The same procedure was followed to prepare supported Pd samples on γ-Al_2O_3 (surface area = 121 $m^2\ g^{-1}$; pore volume = 0.43 $cm^3\ g^{-1}$), as described in ref 3.

Hereafter, we adopted the same nomenclature used in ref 3. PdCw and PdAl is used to indicate the unreduced catalysts prepared on wood carbon (Cw) and alumina (Al), respectively. The Pd loading is indicated before the PdCw label; thus 5PdCw refers to the 5.0 wt % loading. When a pre-reduction is performed, a label indicating the reducing agent is added. Thus, 5PdCw(F), 5PdCw(B), and 5PdCw(H) refer to carbon-supported palladium catalysts (5.0 wt % loading) reduced with formate, borohydride, and hydrogen, respectively; whereas PdAl(F) refers to alumina-supported palladium catalyst reduced with formate. All the Pd supported samples were stored in their wet state. A few samples were reduced in reaction conditions (in ethanol, at 308 K, 1 bar of H_2), but without substrate.

Differently from the results previously obtained on Pd/Al_2O_3 samples, temperature programmed reduction (TPR) data provided evidence that the drying atmosphere greatly affects the properties of the catalysts. In particular, a drying procedure in air resulted often into a Pd^{2+}/Pd_{tot} ratio larger than 1 (as evaluated by TPR measurements). The reason was attributed to a partial oxidation of carbon. As a consequence, the drying step was always conducted in N_2 (unless specified). As demonstrated for PdAl,[3] drying in N_2 does not affect the oxidation state of the supported Pd phase, but causes a downward shift of both T_{start} and T_{max}. This observation is relevant to avoid misleading comparisons with similar data in literature.

Finally, unsupported PdO and Pd samples were prepared as a reference for TPR experiments following a procedure similar to that adopted for the catalyst preparation, but omitting the support. The final unsupported samples were dried overnight in air at 393 K.

2.2. Catalyst Activity in Debenzylation Reaction. The catalytic performance of the Pd/Cw samples was tested in the debenzylation of 4-benzyloxyphenol to hydroquinone and toluene, following the same procedure already described for Pd/Al_2O_3 catalysts. The reaction was carried out in a 300 cm^3 glass reactor equipped with a double mantle for water circulation, and a gas injection stirrer (Premex, br1 series). Water at the required temperature was circulated inside the reactor mantle by means of a thermostatic bath. In a typical experiment, the reactor was charged with 500 mg of dry catalyst, and then a solution of 10 g of 4-benzyloxyphenol in 140 cm^3 of ethanol was poured into the reactor. The reactor was purged first with nitrogen and then with hydrogen. Hydrogenation was performed at atmospheric pressure, at a temperature of 308 K, and with a stirring speed of 2000 rpm. No Pd leaching was observed.

By plotting the hydrogen consumption versus time a straight line is obtained, demonstrating that the reaction has a zero-order with respect to the substrate. The slope of this line corresponds to the activity, expressed in cm^3 STP min^{-1} of consumed H_2. The mean activity of surface Pd atoms can be defined in terms of turnover frequency (TOF), which is the number of H_2 molecules consumed per second per number of surface atoms determined by an independent technique.[20] It was proved that the reaction proceeds without mass transfer constraints in the conditions adopted herein.[3]

2.3. Catalyst Characterization. *2.3.1. TPR and CO Chemisorption.* A Micromeritics Autochem 2910 instrument was used for both TPR and CO chemisorption measurements. For the TPR measurements, the instrument was equipped with a CryoCooler device allowing the measurements to start from 153 K. The water formed during the reduction process was trapped inside a molecular sieve getter located between the sample holder and the detector. A typical procedure was as follows: 100 mg of sample (either wet or dry) are introduced in the sample holder, and heated in situ by a nitrogen flow at 393 K for 2 h.[4,18] Then the sample is cooled down to 153 K under Ar flow (50 $cm^3\ min^{-1}$). Successively, the flow is switched to 5% H_2 in Ar (50 $cm^3\ min^{-1}$) and maintained throughout the analysis. Once a baseline is established, the heating is started at a rate of 5 K min^{-1} up to 623 K. T_{max} and T_{min} indicate the temperatures of the maximum rate of H_2 consumption or release, respectively. T_{start} is the temperature of the beginning of H_2 consumption, defined as the temperature where the first derivative of the TCD signal vs temperature exceeds the threshold value of 5×10^{-4}. Note that all the TPR curves shown hereafter present a minimum around 230 K, which is an instrumental artifact due to a small change in the heating rate.

CO chemisorption measurements were performed at 323 K by a dynamic pulse method on samples pre-reduced in H_2 at 393 K.[21] In a typical experiment, the catalyst (200 mg) was reduced in situ at 393 K according to the following procedure: (i) the catalyst is loaded inside the U-tube, (ii) it is heated in He up to 393 K (heating rate of 10 K min^{-1}), (iii) H_2 is fed for 30 min, and (iv) the sample is cooled down to 323 K in He (cooling rate of 10 K min^{-1}). A CO/Pd average stoichiometry = 1 was assumed to calculate the Pd dispersion. This assumption was verified by measurements performed simultaneously in a static volumetric apparatus on three samples reduced at two different temperatures (393 and 673 K) using both, H_2 and O_2 as probe molecules; these measurements gave a O/Pd average stoichiometry close to 1.[16,22] Comparing the results obtained according to the two methods, a CO/O ratio

dx.doi.org/10.1021/cs400507m | ACS Catal. 2014, 4, 187−194

in the 0.94−1.13 range was obtained, which is a strong support for a CO/Pd average stoichiometry = 1.

2.3.2. X-ray Absorption Spectroscopy (XAS). X-ray absorption experiments at the Pd K-edge (24350 eV) were performed at the BM26A beamline of the ESRF facility (Grenoble, F). The white beam was monochromatized using a Si(111) double crystal; harmonic rejection was performed using Pt-coated silicon mirrors. The following experimental geometry was adopted: (1) I_0 (10% efficiency); (2) sample; (3) I_1 (40% efficiency); (4) reference Pd foil; (5) I_2 (80% efficiency). This setup allows a direct energy/angle calibration for each spectrum avoiding any problem related to little energy shifts due to small thermal instability of the monochromator crystals.[18,23] Extended X-ray absorption fine structure (EXAFS) spectra were collected with a variable sampling step in energy, resulting in Δk = 0.05 Å^{-1}, up to 20 Å^{-1}; the integration time was increased linearly with k from 4 to 25 s/point, to account for the low signal-to-noise ratio at high k values. Both, unreduced and pre-reduced catalysts were measured in the wet form inside a homemade sample holder ad hoc conceived to optimize the sample thickness in the 4−50 mm range, as described elsewhere.[4] To have the correct reference of a completely reduced system, the 5PdCw catalyst was reduced at 393 K in H_2 gas and measured in vacuum, using the in situ EXAFS cell described elsewhere.[24]

For each sample, two consecutive EXAFS spectra were collected, and the corresponding $\chi(k)$ functions were extracted using the Athena code.[25] For each sample, the averaged $k^3\chi(k)$ functions were Fourier Transformed in the Δk = 2.00−15.75 Å^{-1} range.

2.3.3. Transmission Electron Microscopy (TEM). Transmission electron micrographs were obtained using a JEOL 3010-UHR instrument operating at 300 kV, equipped with a 2k × 2k pixels Gatan US1000 CCD camera. Samples were deposited on a copper grid covered with a lacey carbon film.

2.3.4. Small Angle X-ray Scattering (SAXS). SAXS measurements were performed at the DUBBLE beamline BM26A at the European Synchrotron Radiation Facilities (ESRF, Grenoble). The incident 10 keV X-ray beam was monochromatized using the same setup as described above. Samples were placed in a quartz capillary, and the small-angle scattering images were recorded using a two-dimensional MarCCD detector. The resulting scattering vector range was 0.1 < q < 4 nm^{-1}. Silver behenate was used as standard to determine the center of the beam and the scattering vector scale. Then the isotropic SAXS intensity profiles were obtained by integration of the two-dimensional images radially averaged around the center of the primary beam by using FIT2D software.[26−28]

3. RESULTS AND DISCUSSION

3.1. Catalyst Performance in the Debenzylation of 4-Benzyloxyphenol. The catalytic performance of several unreduced catalysts with increasing Pd content were tested in the same debenzylation reaction already employed for the PdAl catalysts, that is the debenzylation of 4-benzyloxyphenol. On the catalyst having a 5 wt % Pd loading, the effect of three different pre-reducing agents was also investigated. Table 1 summarizes the catalytic performance of all the investigated catalysts in terms of induction time and activity.

The same data are shown in Figure 1 and compared to those of PdAl, already discussed in our previous work. The following observations can be made. (i) The induction time (Figure 1a) of PdCw catalysts is significantly lower than for PdAl ones; thus, the supported Pd hydroxide phase is more reducible on carbon than on alumina. In both cases, the induction time decreases upon increasing Pd concentration, and is negligible for pre-reduced catalysts. (ii) The activity (Figure 1b) is higher for PdCw than for PdAl catalysts, and it linearly increases with Pd concentration in both cases. (iii) The pre-reduction has an opposite effect on PdCw and PdAl catalysts: pre-reduced PdCw catalysts display a lower activity than the corresponding unreduced catalyst (black arrow in Figure 1b), whereas an increase in activity is observed for PdAl catalysts (gray arrow in Figure 1b).

Table 1. Catalyst Performance in the Debenzylation of 4-Benzyloxyphenol in Terms of Induction Time[a], and Activity[b] of Unreduced PdCw Catalysts with Different Pd Loading and of 5 wt % Pd-Loaded Catalysts Pre-Reduced with Different Reducing Agents

sample	induction time (min)	activity (cm^3 min^{-1})
0.5PdCw	5.6	1.5
2PdCw	2.7	6.0
3PdCw	3.4	11.8
5PdCw	1.1	16.1
5PdCw(F)	<0.5	13.5
5PdCw(B)	<0.5	12.5
5PdCw(H)	<0.5	13.1

[a]In min. [b]In cm^3 min^{-1} of consumed H_2.

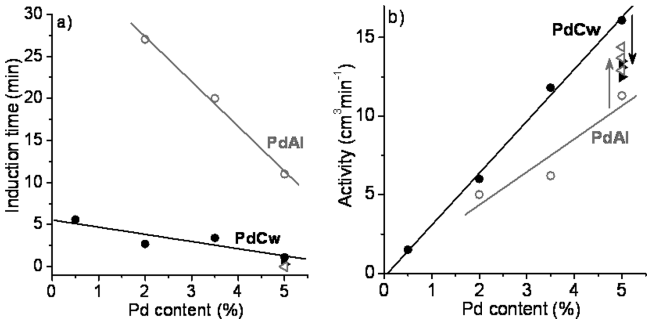

Figure 1. Induction time (part a) and activity (part b) in the debenzylation of 4-benzyloxyphenol by unreduced catalysts having increasing Pd concentration (circles) and 5 wt % pre-reduced catalysts (triangles). Reaction conditions: 308 K, atmospheric pressure, 500 mg of catalyst, and 2000 rpm of stirring speed. Data on PdCw catalysts (black symbols) are summarized in Table 1, whereas data on PdAl (white symbols) are discussed in ref 3. Arrows indicate the effect of pre-reduction on the activity of the 5 wt % catalysts.

The different catalytic performance shown by unreduced PdCw and PdAl suggests that the active phase in the two catalysts has different properties. Moreover, the observation that pre-reduction causes a decrease in the catalytic activity of PdCw, whereas it enhances the catalytic performance of PdAl, suggests that the involved phenomena are different in the two cases. To understand the differences between the two catalyst families, we performed a careful characterization of PdCw catalysts, following the same methodology already employed to characterize PdAl catalysts. The investigation was carried on two steps: (1) characterization of the supported Pd phase in terms of oxidation state, and reducibility; (2) characterization of the Pd nanoparticles obtained after reduction in terms of bulk/surface disorder and aggregation state.

3.2. Oxidation State and Reducibility of the Supported Pd Phase. As previously done for 5PdAl, the first step

dx.doi.org/10.1021/cs400507m | ACS Catal. 2014, 4, 187−194

in the investigation of 5PdCw was the study of the oxidation state and reducibility of the supported Pd phase by the TPR technique. The TPR profiles of both 5PdCw and 5PdCw(F), shown in Figure 2, are quite complex. Both start with a peak at

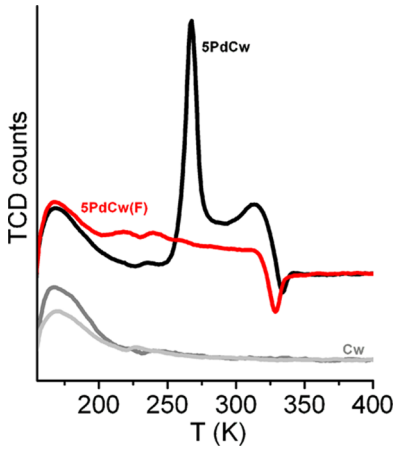

Figure 2. TPR curves of 5PdCw (black) and 5PdCw(F) (red) samples dried in N_2 at 393 K, compared to TPR curves of pure Cw (gray, vertically translated for clarity). Dark gray curve was collected in the same conditions as the TPR of the catalysts (Ar−H_2 flow), whereas the light gray curve was collected after substituting H_2 with the inert He.

very low temperature (T_{max} = 168 K). The same peak is observed in the TPR curve of bare Cw, and therefore it does not involve the Pd phase. In analogy to what has been stated by Sandoval et al.[29] we have hypothesized that this is due to the adsorption of Ar during the stabilization of baseline in 5% H_2−Ar mixture at 150 K; thus, the peak would represent the desorption of Ar with the increasing temperature. We verified this hypothesis by running a TPR of Cw in presence of 5% He−Ar, that is, by substituting hydrogen with helium that has a similar thermal conductivity but is inert. The new profile gave a similar low temperature peak, providing evidence that it is not due to any reduction process, but it is an effect induced by Ar gas.

Besides the low temperature peak, the TPR profile of 5PdCw shows a main peak at T_{max} = 268 K (Figure 2) and a second one at T_{max} = 314 K, both due to the Pd^{2+}→Pd^0 reduction, followed by the negative peak due to the decomposition of the hydride formed at lower temperature. The origin of the two peaks is not yet clear, but it suggests that two types of Pd sites are present on 5PdCw, having a different reducibility. The integrated area below the two positive peaks (after a careful subtraction of the background and correction for both bulk and surface hydride formation) gives the overall hydrogen consumption involved in the reduction process and allows to calculate the Pd^{2+} fraction present in the sample (last column of Table 2). For 5PdCw, Pd^{2+}/Pd_{tot} = 1.03, that means that all the supported Pd is in the Pd^{2+} form within the accuracy of the technique (the Pd^{2+}/Pd_{tot} ratio is determined within ±0.03); therefore, no reduction to Pd^0 occurs during the impregnation step, as already observed in our previous work.[4] This result, already found for 5PdAl, is less straightforward for 5PdCw because the surface chemistry of carbons is very complex and the presence of functional groups that can react with supported PdO cannot be excluded a priori. Moreover, Pd^{2+}→Pd^0 reduction occurs at slightly lower temperature than for PdAl.[3]

Table 2. Summary of the TPR Data Obtained for Un-Reduced and Pre-Reduced 5PdCw Samples Dried in N_2 at 393 K[a]

sample	treatment	T_{start} (K)	T_{max} (K)	Pd^{2+}/Pd_{tot}
PdO	Air 393 K	260	298	1.00
5PdCw	N_2 393 K	250	268	1.03
5PdCw(F)	N_2 393 K	<200	240	0.67
5PdCw(B)	N_2 393 K	<200	232	0.70
5PdCw(H)	N_2 393 K	<200	239	0.67

[a]Also the data obtained for a bulk, unsupported, PdO sample are reported for comparison. T_{start} and T_{max} refer, respectively, to the starting and maximum temperature values of the hydrogen consumption peak due to the Pd^{2+} → Pd^0 reduction; Pd^{2+}/Pd_{tot} is the fraction of Pd^{2+} present in the catalyst.

The TPR profile of 5PdCw(F) is much broader than that of 5PdCw and identification of T_{start} and T_{max} is less straightforward. Nevertheless, the following observations can be made: (i) a fraction of Pd is still oxidized, corresponding to 67% of the total Pd; (ii) reduction of the still oxidized Pd phase starts at lower temperature than for 5PdCw (T_{max} is lowered of 28 K, whereas T_{start} cannot be evaluated because of the interference with the low temperature peak). Similar profiles were obtained for 5PdCw catalysts pre-reduced with other reducing agents: in all the cases, about 70% of the supported Pd phase is still oxidized (data summarized in Table 2).

To confirm that the supported palladium is already partially oxidized in the PdAl(F) catalyst before any drying procedure, XAS data were collected on the same catalysts in the wet form. In our previous work,[4] we already reported a systematic investigation of the EXAFS spectra of unreduced Pd catalysts prepared according to the procedure followed in this work, as a function of the support and of the Pd loading. In all of the investigated samples, the as-precipitated Pd phase was revealed to be an amorphous Pd hydroxide, similar to the Pd^{2+}-polynuclearhydroxo-complexes reported by Troitskii et al.,[30] and no appreciable amount of Pd metal was detected. The supported Pd hydroxide phase is the same found on 5PdAl.[4] This suggests that the higher reducibility of 5PdCw with respect to 5PdAl is due to a different interaction of the Pd phase with the two supports. Thermal treatment in H_2 gas at 393 K caused a full reduction of the Pd^{2+} phase to Pd nanoparticles (as demonstrated also by TPR measurements, PdO in Table 2).

The X-ray absorption near edge structure (XANES) spectra of fresh PdCw, PdCw(F), and of PdCw reduced in H_2 gas are compared in Figure 3a. It is evident that the spectrum of the 5PdCw(F) sample (red) lies in an intermediate position between those of 5PdCw (completely oxidized Pd phase, black) and of the same sample reduced in H_2 gas (completely reduced Pd nanoparticles, gray), confirming that 5PdCw(F) is partially oxidized already in the wet state. The trend is observed in both: (i) the edge position, which upward shifts of about 2 eV by going from 5PdCw to 5PdCw(F) and of other 2 eV going from 5PdCw(F) to 5PdCw reduced in H_2 gas; and (ii) the post-edge range (24370−24400 eV). The partially oxidized state of the 5PdCw(F) sample is qualitatively evident also by looking at Figure 3b, which shows the phase-uncorrected modulus of the FT of the EXAFS signals corresponding to the XANES spectra shown in Figure 3a. The spectrum of 5PdCw (black) displays a Pd−O contribution around 1.6 Å and a double peak around 3.0 Å, which are characteristic of the Pd hydroxide phase.[4] The

dx.doi.org/10.1021/cs400507m | ACS Catal. 2014, 4, 187−194

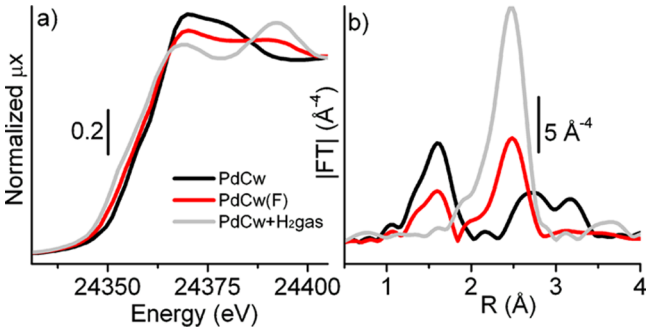

Figure 3. Normalized XANES spectra (part a) and k^3-weighted, phase uncorrected, |FT| of the EXAFS signals (part b), for 5PdCw (black), 5PdCw(F) (red), and 5PdCw reduced in H_2 gas at 393 K (gray).

peak assigned to the Pd−O contribution decreases in intensity for 5PdCw(F) (red), with the attendant growth of a signal around 2.45 Å characteristic of the Pd metal phase (Pd−Pd contribution); this peak, however, has an intensity which is only half of that obtained upon full reduction of 5PdCw in H_2 gas (gray).

In principle, the XANES and EXAFS spectra shown in Figure 3 could be potentially exploitable to quantitatively determine the reduction degree of the Pd phase in 5PdCw(F), that is, the relative fraction of Pd^{2+} and metal Pd, thus obtaining the same information as those obtained by TPR. As a matter of fact, two-phase problems in XAS spectroscopy can be solved in a highly accurate way, provided that a proper standard spectrum for each independent phase is available.[18,23,31−36] Unfortunately, this is not the present case, for three main reasons. (1) The choice of the reference spectrum for the Pd^0 phase is difficult when dealing with metal nanoparticles, because it is well-known that the fraction of metal Pd strongly correlates with the particle dimension in determining the amplitude of the characteristic Pd−Pd peak.[19,37−40] (2) Likewise, the choice of a reference spectrum for the Pd^{2+} phase is critical. While the spectrum of 5PdCw could be well used as a reference for Pd-hydroxide nanoparticles, it is not exploitable to simulate the contribution of a few monolayers of PdO. On the other hand, bulk PdO is typically obtained at high temperature and therefore it is intrinsically much more ordered than a few monolayers of PdO,[41,42] with important consequences in the EXAFS signal. (3) The contribution from the Pd^{2+}/Pd^0 interface is highly relevant and cannot be neglected in a quantitative data analysis. All these reasons precluded a quantitative evaluation of the Pd^{2+} fraction present in the 5PdCw(F) catalyst from XAS data. Nevertheless, both XANES and EXAFS data shown in Figure 3 confirm that in the 5PdCw(F) catalyst a relevant fraction of the Pd phase is in the oxidized form, even when the sample is in the wet state; Pd is fully reduced only in the catalysts reduced in situ by H_2 gas.

The TPR and XAS data discussed above provide evidence that after pre-reduction the Pd phase supported on Cw is still partially oxidized; however, this oxidized phase is more easily reducible than that on unreduced 5PdCw. The same conclusions were drawn for PdAl catalysts, for which it was demonstrated that, although Na-formate fully reduces the supported Pd-hydroxide phase, the resulting Pd^0 is partially reoxidized by air on both surface and subsurface layers. In spite of the fact that reoxidation has been observed on both supports, we have found that pre-reduction has an opposite effect on the catalytic performance of PdCw and PdAl catalysts (see Figure 1 and Table 1); therefore, it should be hypothesized that it plays a different role in defining the properties of the reduced Pd nanoparticles obtained on different supports.

3.3. Properties of Reduced Pd. Following the conclusion of the previous paragraph, we investigated the properties of the 5PdCw catalysts after formation of Pd nanoparticles in reducing conditions. To this aim, both unreduced and pre-reduced 5PdCw catalysts were fully reduced in H_2 gas at 393 K. The Pd dispersion (i.e., the ratio between surface and total metal atoms) was evaluated by means of two independent techniques: (i) CO chemisorption, which measures the number of adsorbed CO molecules and, under the assumption of a defined CO/Pd stoichiometry, provides the fraction of available surface Pd atoms; (ii) SAXS, which gives a particle size distribution on the whole particle population. We have previously demonstrated[3] that the coupling of these two techniques is necessary to discriminate between poisoning phenomena of the exposed metal surface and increase of the particle size, both cases causing a decrease of the dispersion values. The Pd dispersion as obtained by CO chemisorption (D_{Chemi}) and by SAXS (D_{SAXS}) on the different 5PdCw catalysts reduced in H_2 gas at 393 K are summarized in Table 3; in Figure 4 the same data are compared with those previously obtained on 5PdAl. Both techniques revealed that Pd particles in unreduced 5PdCw have a lower dispersion than on unreduced PdAl, suggesting that the average particle size is larger. However, opposite to the 5PdAl case, on 5PdCw the effect of pre-reduction on the Pd dispersion is negligible. The agreement between CO chemisorption (black filled bars in Figure 4a, top) and SAXS data (dashed bars in Figure 4a, top) provides evidence that during pre-reduction of 5PdCw neither sintering of Pd particles nor embedding into the carbon support occur, both phenomena being observed for 5PdAl (see discrepancy between gray filled and dashed bars in Figure 4a, bottom).

Table 3. Pd Dispersion As Obtained by CO Chemisorption Data (D_{Chemi}) and by SAXS Data (D_{SAXS}), Minimum of the Negative Peak Due to the Decomposition of Pd Hydride (T_{min}), and the Corresponding H/Pd in Pd Hydride, As Obtained by TPR[a]

sample	D_{Chemi} (%)	D_{SAXS} (%)[b]	T_{min} (K)	H/Pd in Pd hydride
bulk Pd	0.2		339	0.50
5PdCw	24.4	23.9 (24.6)	325	0.24
5PdCw(F)	23.5	23.3 (21.3)	326	0.22
5PdCw(H)	23.2	23.0 (21.5)	326	0.24

[a]All the values refer to samples that were reduced in H_2 at 393 K before the measurement, except for the values reported in brackets in the D_{SAXS} column, that refer to the sample measured before H2 reduction. [b]D_{SAXS} is calculated starting from particle size distribution by SAXS, considering particles with cuboctahedral shape and with 1/6 of their surface in contact with the support.[16]

As discussed in our previous work,[3] complementary information on the Pd dispersion can be obtained by analysis of TPR data in the hydride region. As a matter of fact, the H/Pd ratio and the decomposition temperature of the hydride depend on both the Pd dispersion and the internal disorder of the Pd particles, being the two factors often correlated each others. Generally, the lower the H/Pd ratio, and the lower the temperature of the hydride decomposition, the more disordered the Pd particles. As summarized in Table 3 (last two columns) and shown in Figure 4b,c (top), for 5PdCw both

dx.doi.org/10.1021/cs400507m | ACS Catal. 2014, 4, 187−194

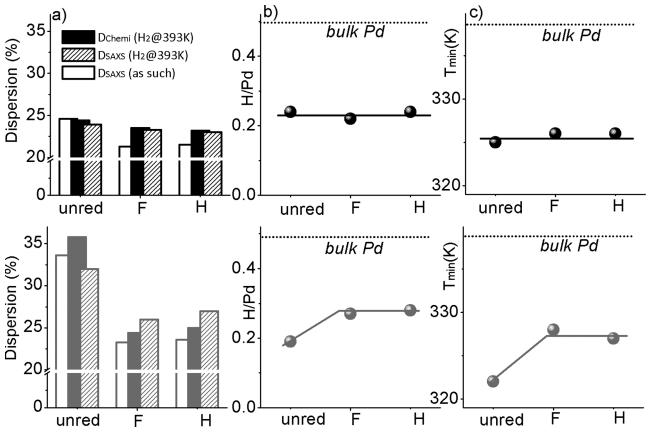

Figure 4. (a) Pd dispersion as obtained by CO chemisorption data (D_{Chemi}, filled bars) and by SAXS data collected on samples reduced in H_2 at 393 K (dashed bars) and on samples as such (white bars). (b) H/Pd ratio in Pd hydride as obtained by TPR. (c) Minimum of the negative peak due to the decomposition of the formed Pd hydride, T_{min}, as obtained by TPR. Top parts refer to 5PdCw samples (data summarized in Table 3), whereas bottom parts refer to 5PdAl samples (data discussed in ref 3 herein multiplied by a factor 5/6 to roughly take into account for the fraction of Pd surface not available for CO adsorption because in contact with the support).

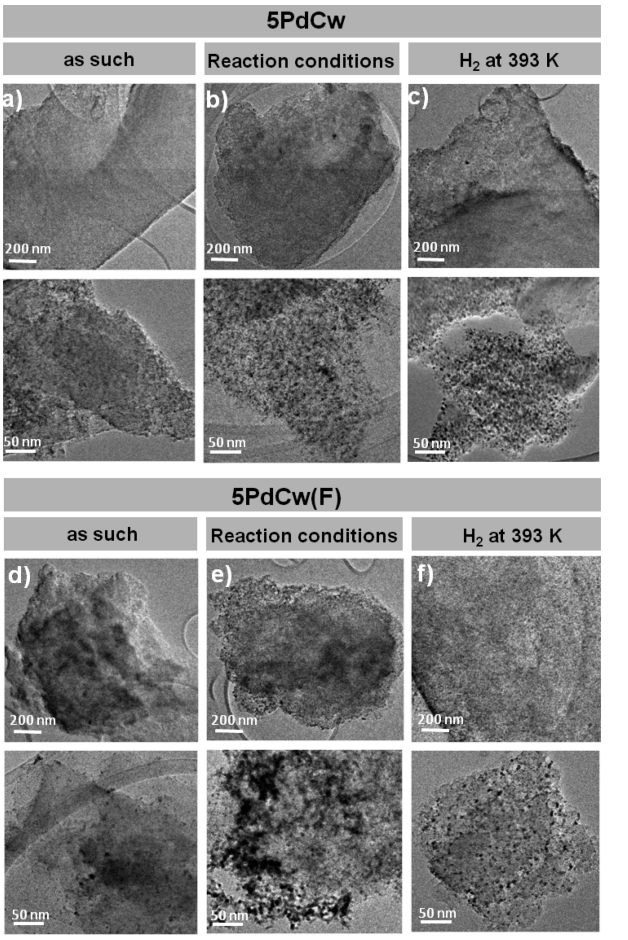

Figure 5. Selected TEM micrographs at very low (top) and low (bottom) magnification of 5PdCw and 5PdCw(F) catalysts as such or subjected to different treatments. Reported micrographs are representative of the situation observed on a large number of micrographs. By reaction conditions we meant 1 bar of H_2 at 308 K in ethanol without substrate.

T_{min} and H/Pd ratio are not influenced by pre-reduction procedure, suggesting that the formed Pd nanoparticles have not only the same dispersion (in agreement with CO chemisorption data) but also a similar bulk order. On the contrary, the H/Pd ratio and T_{min} of 5PdAl increased after pre-reduction (Figure 4b,c, bottom).

The results obtained with three independent techniques undoubtedly point out that pre-reduction does not affect the properties of the carbon-supported Pd particles in terms of particle size, available surface sites, and bulk order. Nevertheless, the 5PdCw pre-reduced catalysts must be different from the unreduced one to account for the different catalytic performance. Taking into account the possibility that the reduction in H_2 gas does not reproduce the reaction conditions, we have performed additional measurements on the catalysts as such (i.e., before any reduction in the gas phase) both unreduced and pre-reduced, as reported in the next paragraph.

3.4. Aggregation State of the Pd Particles. In the attempt to understand the origin of the different catalytic performance shown by unreduced and pre-reduced 5PdCw catalysts, we carried out a detailed TEM investigation on the samples as such, that is, not reduced in H_2 gas at 393 K. The images were collected at low magnification to detect the presence of aggregates of Pd particles on a micrometric scale. A selection of representative pictures is shown in Figure 5. TEM images at low magnification immediately reveal the presence of aggregated Pd particles in the pre-reduced catalyst (Figure 5d), which are not present in the unreduced one (Figure 5a). This means that during pre-reduction the Pd particles move on the support and agglomerate together. This phenomenon is peculiar of carbon-supported catalysts, since it was not observed for 5PdAl, and reveals that interaction of the Pd-phase with the support is lower for carbon than for alumina. The exposure of samples as such to reaction conditions does not change the aggregation degree of Pd particles, that remains negligible on unreduced samples (Figure 5b) and relevant on pre-reduced ones (Figure 5e): the data collected on samples as such are thus representative of the particle properties in reaction conditions. On the contrary, reduction in H_2 gas at 393 K drastically decreases the amount of aggregated particles in PdCw(F) (Figure 5f); accordingly, the same treatment does not change the negligible aggregation degree of the Pd particles in unreduced 5PdCw (Figure 5c).

TEM analysis allows the following preliminary conclusions to be drawn: (i) pre-reduction promotes aggregation of Pd particles; (ii) samples as-such are representative of the status of the Pd particles in reaction conditions; (iii) a treatment in H_2 gas at 393 K modifies the samples, because it causes the destruction of the Pd aggregates. Therefore, the dispersion values of Pd particles in pre-reduced catalysts as obtained by CO chemisorption and TPR are not representative of the Pd dispersion in reaction conditions, since both techniques require a treatment of the investigated samples in H_2 gas before the measurements. The same problem is present for the SAXS data discussed in the previous paragraph (third column in Table 3 and dashed bars in Figure 4a), because they were collected on samples treated in the same way as for CO chemisorption and TPR measurements. It is clear from this TEM study that reliable Pd dispersion values for pre-reduced catalysts can be obtained only by means of techniques that do not require a treatment of the samples in H_2 gas.

dx.doi.org/10.1021/cs400507m | ACS Catal. 2014, 4, 187−194

High resolution TEM could potentially offer the possibility to evaluate the particle size distribution for samples as such. However, in the presence of aggregates or embedding phenomena, the determination of the particle borders becomes arbitrary. Moreover, it is well-known that particles smaller than about 1 nm escape detection by standard TEM instruments, and that the analysis is performed only on a small fraction of the whole particle population. For these reasons, we turned our attention to SAXS, which can be applied also on samples not treated in H_2 gas; the goal of the new set of measurements was to verify if the aggregation of Pd particles observed on a micrometric scale by TEM corresponds to an aggregation also on a nanometric scale. Some representative particle size distributions are shown in Figure 6. As already discussed in

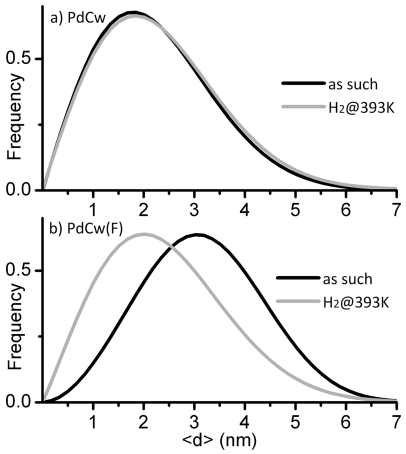

Figure 6. Particle size distribution for 5PdCw (part a) and 5PdCw(F) (part b) obtained by SAXS analysis on samples as such (black curves) and treated in H_2 at 393 K (gray curves).

the previous paragraph, after reduction in H_2 gas the Pd particle size distribution is the same for 5PdCw and 5PdCw(F) (gray curves in Figure 6), thus resulting in similar dispersion values. However, a large difference is observed in the particle size distribution of the two samples as such (black curves in Figure 6). While the curve for 5PdCw as such is perfectly overlapped to that of the same sample treated in H_2 at 393 K (Figure 6a), that of 5PdCw(F) as such is shifted to higher diameter values (Figure 6b). The resulting dispersion values, summarized in Table 3 (third column, values in brackets) and shown in Figure 4a (white histograms) are the most representative of the Pd dispersion in reaction conditions.

3.5. Correlation between Catalyst Properties and Catalytic Performance. The SAXS data shown in Figure 6 provide a clear evidence that, in reaction conditions, the pre-reduced 5PdCw catalysts are characterized by a lower Pd dispersion than the corresponding unreduced catalyst. Therefore, more reliable TOF values could be calculated on the basis of dispersion measured by SAXS rather than CO chemisorption. Figure 7 reports the TOF values evaluated as the number of H_2 molecules consumed per second per number of surface atoms, as determined from CO chemisorption (part a) and from SAXS data collected on samples as such (part b), for unreduced (circles) and pre-reduced (triangles) 5PdCw and 5PdAl catalysts.

It is evident that the TOF vs dispersion trend for 5PdAl (gray arrows in Figure 7) is the same whichever is the method used to evaluate the dispersion (only small variations in the absolute

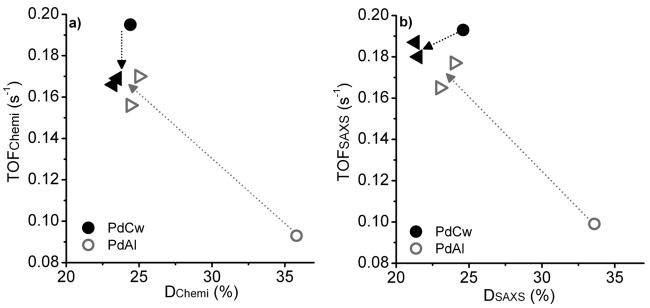

Figure 7. Turnover frequency (TOF, s^{-1}) in the debenzylation of 4-benzyloxyphenol, defined as the number of H_2 molecules consumed per second per number of surface atoms, as determined from CO chemisorption (part a) and from SAXS data collected on samples as such (part b), for unreduced (circles) and pre-reduced (triangles) 5PdCw (black) and 5PdAl (white) catalysts. The arrows evidence the TOF vs dispersion trend induced by pre-reduction.

values are observed): pre-reduction causes a remarkable decrease in particle dispersion (about 30%) and a relevant increase in TOF (about 70%). We attributed this behavior to the fact that pre-reduced Pd particles are slightly larger and more regular than unreduced ones, and thus favor a structure sensitive reaction such as the debenzylation of 4-benzyloxyphenol. On the contrary, the TOF vs dispersion trend for 5PdCw catalysts (black arrows in Figure 7) is different when the Pd dispersion is evaluated by CO chemisorption (part a) or SAXS (part b). According to the first technique, pre-reduction causes a decrease in TOF (of about 13%) that is not accompanied by any change in dispersion, neither in a change of any other particle property, and thus is difficult to be explained. When dispersion and TOF values are determined from SAXS data, it comes out that pre-reduction causes a decrease of particle dispersion (about 13%), which accounts for a small decrease of TOF values (less than 10%). TEM and SAXS data provided evidence that the lower Pd dispersion is a consequence of the movement and aggregation of Pd particles on the carbon support, promoted by the liquid reducing medium and by the negligible interaction between the Pd phase and the carbon support; whereas the aggregates are destroyed by reduction in H_2 gas.

4. CONCLUSIONS

A systematic investigation, by means of a multitechnique approach, was carried out on Pd/carbon catalysts (5PdCw) to determine the role of pre-reduction in solution with chemical reagents in affecting the catalytic performance and the catalyst properties. The results were critically discussed in comparison with those recently obtained on Pd/alumina catalysts (5PdAl). The following was found.

(1) Both 5PdAl and 5PdCw pre-reduced catalysts are more easily reducible in reaction condition (negligible induction time), although more than 50% of the Pd phase is still oxidized.

(2) Pre-reduction greatly affects the properties of the final Pd particles in 5PdAl samples, in terms of particle size and regularity; the sum of all these effects accounts for a relevant increase in TOF. On the contrary, in PdCw the effects of pre-reduction on the properties of the final Pd particles in terms of size and regularity are negligible, whereas the liquid reducing medium promotes an aggregation of the Pd particles on the carbon support, with a consequent decrease of available metal surface. The consequence in terms of catalytic performance is a

dx.doi.org/10.1021/cs400507m | ACS Catal. 2014, 4, 187−194

decrease in TOF values. By comparing the results obtained on 5PdAl and 5PdCw it can be stated that catalytic performance in the debenzylation of 4-benzyloxyphenol is affected by Pd particle size and regularity much more than by particle aggregation state.

(3) The mobility of the Pd phase is much higher in carbons than on alumina; therefore, Pd particle aggregation can be observed on carbons, depending on the activation conditions. In these cases, care must be taken in analyzing the data obtained by means of techniques that require an activation procedure in H_2 gas (such as CO chemisorption and TPR).

AUTHOR INFORMATION

Corresponding Author

*E-mail: agostini@esrf.fr. Phone: +33 (0)4 38 88 1914.

Notes

The authors declare no competing financial interest.

ACKNOWLEDGMENTS

We are indebted to the whole staff of DUBBLE BM26 beamline at the ESRF (particularly to Daniel Hermida Merino, S. Nikitenko, G. Portale, and W. Brass) where both Pd K-edge EXAFS and SAXS measurements were performed. We are particularly grateful to Andrea Governini (Chimet SpA) for the catalytic activity measurements and to Massimo Graziani (Chimet SpA) for the chemisorption measurements. This work has been supported by "Progetti di Ricerca di Ateneo-Compagnia di San Paolo-2011-Linea 1A, ORTO11RRT5 project".

REFERENCES

(1) Blaser, H.-U.; Siegrist, U.; Steiner, H. In *Fine Chemicals through Heterogeneous Catalysis*; Sheldon, R. A., van Bekkum, H., Eds.; Wiley-VCH: Weinheim, Germany, 2001; p 389.

(2) Auer, E.; Freund, A.; Pietsch, J.; Tacke, T. *Appl. Catal., A* **1998**, *173*, 259−271.

(3) Groppo, E.; Agostini, G.; Piovano, A.; Muddada, N. B.; Leofanti, G.; Pellegrini, R.; Portale, G.; Longo, A.; Lamberti, C. *J. Catal.* **2012**, *287*, 44−54.

(4) Agostini, G.; Groppo, E.; Piovano, A.; Pellegrini, R.; Leofanti, G.; Lamberti, C. *Langmuir* **2010**, *26*, 11204−11211.

(5) Markus, H.; Plomp, A. J.; Maki-Arvela, P.; Bitter, J. H.; Murzin, D. Y. *Catal. Lett.* **2007**, *113*, 141−146.

(6) Venezia, A. M.; La Parola, V.; Pawelec, B.; Fierro, J. L. G. *Appl. Catal., A* **2004**, *264*, 43−51.

(7) Ruta, M.; Semagina, N.; Kiwi-Minsker, L. *J. Phys. Chem. C* **2008**, *112*, 13635−13641.

(8) Ruta, M.; Laurenczy, G.; Dyson, P. J.; Kiwi-Minsker, L. *J. Phys. Chem. C* **2008**, *112*, 17814−17819.

(9) Min, K.-I.; Choi, J.-S.; Chung, Y.-M.; Ahn, W.-S.; Ryoo, R.; Lim, P. K. *Appl. Catal., A* **2008**, *337*, 97−104.

(10) Okhlopkova, L. B.; Lisitsyn, A. S.; Likholobov, V. A.; Gurrath, M.; Boehm, H. P. *Appl. Catal., A* **2000**, *204*, 229−240.

(11) Pearlman, W. M. *Tetrahedron Lett.* **1967**, *8*, 1663−1664.

(12) Griffin, K. G.; Hawker, S.; Batti, M. A. In *Catalysis of organic Reactions*; Malz, R. E., Ed.; Marcel Dekker, Inc.: New York, 1996; pp 325−334.

(13) Blaser, H.-U.; Indolese, A.; Schnyder, A.; Steiner, H.; Studer, M. *J. Mol. Catal. A: Chem.* **2001**, *173*, 3−18.

(14) Markus, H.; Plomp, A. J.; Sandberg, T.; Nieminen, V.; Bitter, J. H.; Murzin, D. Y. *J. Mol. Catal. A: Chem.* **2007**, *274*, 42−49.

(15) Galletti, A. M. R.; Bonaccorsi, F.; Calvani, F.; Di Bugno, C. *Catal. Commun.* **2006**, *7*, 896−900.

(16) Agostini, G.; Pellegrini, R.; Leofanti, G.; Bertinetti, L.; Bertarione, S.; Groppo, E.; Zecchina, A.; Lamberti, C. *J. Phys. Chem. C* **2009**, *113*, 10485−10492.

(17) Pellegrini, R.; Leofanti, G.; Agostini, G.; Rivallain, M.; Groppo, E.; Lamberti, C. *Langmuir* **2009**, *25*, 6476−6485.

(18) Pellegrini, R.; Leofanti, G.; Agostini, G.; Bertinetti, L.; Bertarione, S.; Groppo, E.; Zecchina, A.; Lamberti, C. *J. Catal.* **2009**, *267*, 40−49.

(19) Groppo, E.; Liu, W.; Zavorotynska, O.; Agostini, G.; Spoto, G.; Bordiga, S.; Lamberti, C.; Zecchina, A. *Chem. Mater.* **2010**, *22*, 2297−2308.

(20) Boudart, M. *Chem. Rev.* **1995**, *95*, 661−666.

(21) Anderson, J. R.; Pratt, K. C. In *Introduction to Characterization and Testing of Catalysts*; Academic Press: Sydney, Australia, 1986; pp 1−53.

(22) Prelazzi, G.; Cerboni, M.; Leofanti, G. *J. Catal.* **1999**, *181*, 73−79.

(23) Lamberti, C.; Bordiga, S.; Bonino, F.; Prestipino, C.; Berlier, G.; Capello, L.; D'Acapito, F.; Llabres i Xamena, F. X.; Zecchina, A. *Phys. Chem. Chem. Phys.* **2003**, *5*, 4502−4509.

(24) Lamberti, C.; Prestipino, C.; Bordiga, S.; Berlier, G.; Spoto, G.; Zecchina, A.; Laloni, A.; La Manna, F.; D'Anca, F.; Felici, R.; D'Acapito, F.; Roy, P. *Nucl. Instrum. Meth. B* **2003**, *200*, 196−201.

(25) Ravel, B.; Newville, M. *J. Synchrotron Radiat.* **2005**, *12*, 537−541.

(26) Hammersley, A. P. *FIT2D*; 1998.

(27) Longo, A.; Calandra, P.; Casaletto, M. P.; Giordano, C.; Venezia, A. M.; Turco Liveri, V. *Mater. Chem. Phys.* **2006**, *96*, 66−72.

(28) Cattaruzza, E.; D'Acapito, F.; Gonella, F.; Longo, A.; Martorana, A.; Mattei, G.; Maurizio, C.; Thiaudière, D. *Appl. Crystallogr.* **2000**, *33*, 740−743.

(29) Sandoval, V. H.; Gigola, C. E. *Appl. Catal., A* **1996**, *148*, 81−96.

(30) Troitskii, S. Y.; Chuvilin, A. L.; Kochubei, D. I.; Novgorodov, B. N.; Kolomiichuk, V. N.; Likholobov, V. A. *Russ. Chem. Bull.* **1995**, *44*, 1822−1826.

(31) Piskorska, E.; Lawniczak-Jablonska, K.; Minikayev, R.; Wolska, A.; Paszkowicz, W.; Klimczyk, P.; Benko, E. *Spectrochim. Acta, Part B* **2007**, *62*, 461−469.

(32) Le Toquin, R.; Paulus, W.; Cousson, A.; Prestipino, C.; Lamberti, C. *J. Am. Chem. Soc.* **2006**, *128*, 13161−13174.

(33) Groppo, E.; Prestipino, C.; Cesano, F.; Bonino, F.; Bordiga, S.; Lamberti, C.; Thune, P. C.; Niemantsverdriet, J. W.; Zecchina, A. *J. Catal.* **2005**, *230*, 98−108.

(34) Prestipino, C.; Bordiga, S.; Lamberti, C.; Vidotto, S.; Garilli, M.; Cremaschi, B.; Marsella, A.; Leofanti, G.; Fisicaro, P.; Spoto, G.; Zecchina, A. *J. Phys. Chem. B* **2003**, *107*, 5022−5030.

(35) Lamberti, C.; Prestipino, C.; Bonino, F.; Capello, L.; Bordiga, S.; Spoto, G.; Zecchina, A.; Moreno, S. D.; Cremaschi, B.; Garilli, M.; Marsella, A.; Carmello, D.; Vidotto, S.; Leofanti, G. *Angew. Chem., Int. Ed.* **2002**, *41*, 2341−2344.

(36) Ressler, T.; Wienold, J.; Jentoft, R. E.; Neisius, T.; Gunter, M. M. *Top. Catal.* **2002**, *18*, 45−52.

(37) Stern, E. A.; Siegel, R. W.; Newville, M.; Sanders, P. G.; Haskel, D. *Phys. Rev. Lett.* **1995**, *75*, 3874−3877.

(38) Boscherini, F.; de Panfilis, S.; Weissmuller, J. *Phys. Rev. B* **1998**, *57*, 3365−3374.

(39) Frenkel, A. I. *J. Synchrotron Radiat.* **1999**, *6*, 293−295.

(40) Frenkel, A. I.; Hills, C. W.; Nuzzo, R. G. *J. Phys. Chem. B* **2001**, *105*, 12689−12703.

(41) Ugarl, P.; Hilaire, L.; Maire, G.; Krill, G.; Amamou, A. *Surf. Sci.* **1981**, *107*, 533.

(42) Kim, K. S.; Gossmann, A. F.; Winograd, N. *Anal. Chem.* **1974**, *46*, 197.